An influenza epidemic model with dynamic social networks of agents with individual behaviour

Leonardo López[a,*], Maximiliano Fernández[b], Andrea Gómez[c], Leonardo Giovanini[b]

[a]*Barcelona Institute for Global Health, Barcelona, Spain*
[b]*Research Institute for Signals, Systems and Computational Intelligence, sinc(i), FICH-UNL-CONICET, Argentina*
[c]*National Scientific and Technical Research Council, CONICET, Argentina*

Abstract

There is an interplay between the spread of infectious disease and the behaviour of individuals that can be modelled through a series of interconnected dynamical feedback blocks. Specifically, the outbreak of an infectious disease can trigger behavioural responses, at the group and individual levels, which in turn influences the epidemic evolution. Daily life interactions can be modelled through adaptive co-evolutionary networks whose nodes represent the interconnected individuals. In this paper we introduce an individual-based model where the behaviour of each agent is determined by both external stimuli and perception of its environment. It is built as a combination of three interacting blocks that model the fundamental aspects of an epidemic: i) individual behaviour, ii) social behaviour and iii) health state.

Keywords: Individual-Based Model; Adaptive Co-evolutionary Networks; Fuzzy-Cognitive Maps; Infectious Disease

1. Introduction

Since the first mathematical approach to the spread of a disease [1], epidemic models lie at the core of the understanding infectious diseases. Because of experimenting *in-vivo* is not an available option, modelling approaches have been the main resource to compare and test theories. Therefore, epidemic modelling is a research field that crosses different disciplines and develops a wide variety of approaches [2]. The integration of large-scale data sets with explicit simulations of entire populations has improved the accuracy of epidemiological studies [3, 4, 5, 6, 7, 8]. Many mathematical and computational models have evolved to include spatial structures, individual heterogeneity and multiple time-scales in the evolution of epidemics [9, 10, 11], among other topics.

The core of epidemic modelling approaches dwells on the structure of human interactions, mobility and contact patterns, which can be represented through networks. The key element

*I am corresponding author
Email address: leonardorafael.lopez@isglobal.org (Leonardo López)

to understand this dynamic is the comprehension of the interplay between epidemics processes, individual behaviour and networks dynamics. Epidemic spreading in real world networks is different from regular lattices. A large number of works have shown that real-world networks show dynamic self-organization and they are statistically heterogeneous, which are typical features of complex systems [12, 13]. Networks are hierarchically organized with few nodes having a large number of interactions and the majority of them having few interactions. This hierarchical structure implies a network organization in communities of tightly interconnected nodes. Another difference between theoretical and real-world networks is the connection process, which is determined by organizing principles and correlations, defining the network structure and the evolution of contagion process.

In this paper we introduce a modelling framework where the individual is the basic modelling unit and the system dynamics arises from the aggregation of individuals behaviour. The individual behaviour is the key to understand the epidemiological system. It determines how individuals unfold in the environment, and hence defines the epidemic dynamics. We propose to model the individual behaviour using a modular approach based on interacting blocks: *i*) individual behaviour, *ii*) social behaviour and *iii*) health state. The paper is organized as follows: Section 2 shows a general description of the model. Section 3 provides details on a selected case of study and it discusses the results. Subsection 3.1 describes the way in which the model was implemented for modelling a Spanish flu epidemic. Subsection 3.2 shows the parameter's estimation of the proposed model. Subsection 3.4 shows and analyzes the results obtained with the model. Finally, Section 4 summarizes the conclusions of this work.

2. Framework Description

The interrelation between the spread of infectious disease and individual behaviour is the result of dynamical feedback blocks between perceptions, experiences, social behaviour and disease evolution. Specifically, an infectious disease outbreak can trigger behavioural responses (at the group and individual levels) that influence the evolution of epidemics. To develop models where disease dynamics and social behaviour are intertwined, we need to incorporate the mechanisms behind this mutual influence answering questions like: To what extent do people, their social group, media opinion and personal perceptions influence individual behaviour? and which are the features of infections that influence, through perceptions, the individual behaviour? Following the idea introduced by Gross et al. [14], we propose a modelling framework based on adaptive co-evolutionary networks where the interplay between epidemic dynamic and temporal evolution of network structure is assimilated. The individual–based model is built upon agents whose behaviour emerge from the interactions of three intertwined components: *i)* Individual behaviour, *ii)* social behaviour and *iii)* health state.

The idea behind this decomposition is to facilitate the description of the system and to elucidate the relationship between individual behaviour and disease spreading. Besides, the modular structure of the agent's behaviour allows to use different tools for each component. The agent's behaviour is modelled with:

sinc(*i*) Research Institute for Signals, Systems and Computational Intelligence (sinc.unl.edu.ar)
L. López, M. Fernández, A. Gómez & L. Giovanini; "An influenza epidemic model with dynamic social networks of agents with individual behaviour"
Ecological Complexity, Vol. 41, 2020.

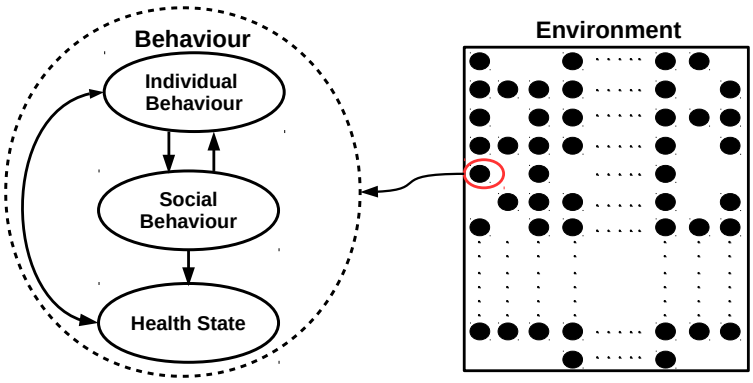

Figure 1: Model diagram showing the different components of individual behaviour and relationships.

i) **Individual behaviour** determines how an agent reacts to external stimuli that influence its behaviour like communication, cultural norms and personal circumstances, among others. It involves subjective experience, cognitive processes and instrumental behavior, given by a combination of emotions, perceptions, memories and logical reasoning that result in physical and emotional changes. It promotes acceptable adaptive responses to recurrent problems that individuals face every day [15];

ii) **Social behaviour** determines how individuals establish relationships with others. It is given by intraspecific relationships like communication and social practices. It is regulated by the individual behaviour and it is modified by the environment where the agent lies in. Depending on the problem under study, social behaviour can explicitly model the physical space or any other relevant space like social connections; and

iii) **Health state** determines the evolution of agent's health state along the disease evolution. The epidemiological analysis must consider the structure, epidemiological characteristics and behaviour of the disease.

It is clear that there are feedback interactions between social and individual behaviour. Individuals interact with others, modifying their perceptions and experiences that in turn make them react in ways that modify the group dynamic. The presence of a disease modifies the behaviour of each individual, changing the structure of the groups. Figure 2 shows the

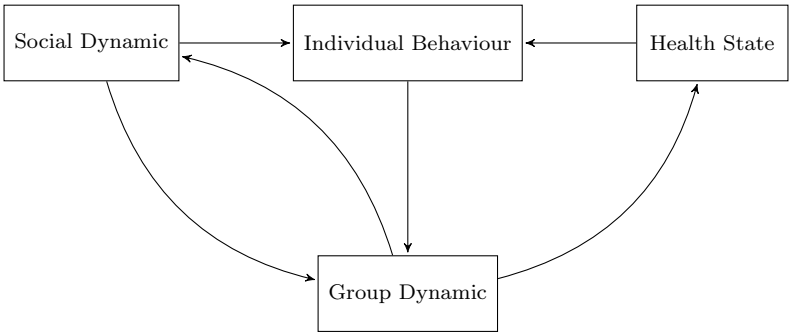

Figure 2: Adaptive network scheme.

sinc(*i*) Research Institute for Signals, Systems and Computational Intelligence (sinc.unl.edu.ar)
L. López, M. Fernández, A. Gómez & L. Giovanini; "An influenza epidemic model with dynamic social networks of agents with individual behaviour"
Ecological Complexity, Vol. 41, 2020.

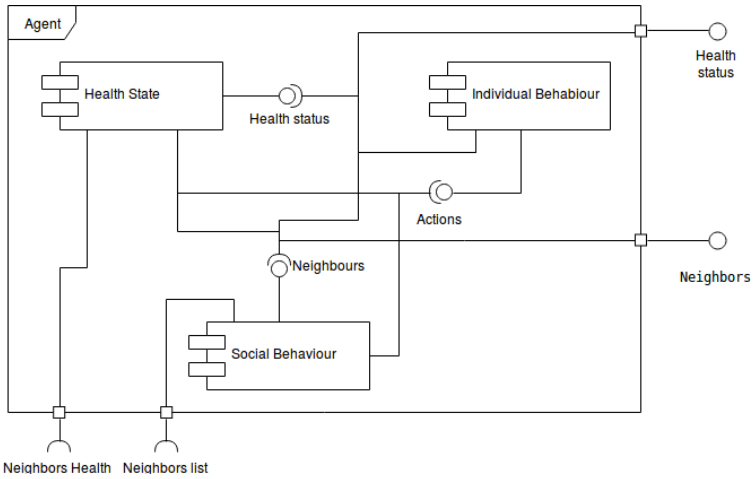

Figure 3: UML diagram showing the components and connections of the framework.

diagram of these relationships. The evolution of the network topology depends on the nodes dynamic, creating feedback loops between the group (the network topology close to the individual) and social (the topology of the entire network) dynamic.

Figure 3 shows the connection between the blocks use to model the behaviour and the connections with other agents. The proposed framework links the macro level (population behaviour) with the micro level (individual behaviour) using the aggregation of agents described in previous paragraphs. The behaviour of each agents modifies their neighbourhood by interacting with the others agents. Then, the group behaviour is the result of the aggregation of all agents of the group. Following the same mechanism, the behaviour of a sub-population is obtained by the aggregation of smaller groups, and then the entire population.

2.1. Individual behaviour

Human behaviour is affected by countless factors ranging from media and person-to-person communication to emotions and perceptions. The behaviour towards an infectious disease is determined by a combination of these factors. Different models had been proposed to imitate this dynamic, such as *SOAR* [16], *ACT-R* [17], *EMA* [18] or *FMC* [19]. Human emotions can be classified, according to their temporal scale into [19]:

i) **Primary emotions** are the individual intrinsic response to external stimuli;
ii) **Secondary emotions** are activated when the primary emotions are connected with previous experiences (memories) and past perception; and
iii) **Senior emotions** are produced by the course of long-term social contacts in a given environment [15].

This mental processing can be represented through a cognitive map that comprises cognitive abstractions by which individuals filter, store and recall information about experiences [20]. Fuzzy Cognitive Maps (*FCM*) provide a tool for modelling complex systems, like mental processing, in terms of interacting concepts. They use concepts to represent states and links

sinc(*i*) Research Institute for Signals, Systems and Computational Intelligence (sinc.unl.edu.ar)
L. López, M. Fernández, A. Gómez & L. Giovanini; "An influenza epidemic model with dynamic social networks of agents with individual behaviour"
Ecological Complexity, Vol. 41, 2020.

to model causal relationship through a hierarchical graph that shows the cause and effect relationships between concepts. Connections between concepts are characterized by a weight $w_{ij} \in [-1, 1]$ that quantifies the degree of causality between the concepts C_i and C_j. The sign indicates the type of causality: $w_{ij} > 0$ indicates positive causality between C_i and C_j, if C_i increases then C_j also increases, while $w_{ij} < 0$ indicates negative causality, if C_i increases then C_j decreases. When there is no relationship between the concepts $w_{ij} = 0$. The value of each weight w_{ij} is estimated by computing the influence of concepts on a specific one [21, 22].

2.2. Social behaviour

Social behaviour determines how individuals relate with others, establishing the structure and dynamic of social network along time. It is regulated by agent individual behaviour, since the social behaviour is the result of agents' actions based on its perceptions and health state. It can be modelled through a network model (a graph of individuals and their relationships), providing a framework where connections between individuals are more relevant than the network topology itself. Network models describe the relationships between individuals specifying the connections between nodes and quantifying the mutual influence. The network configuration, at any time t, is an aggregation of nodes' states and network topology. Formally it is defined by:

- $\mathcal{V}_t$ is a finite set of nodes $v_{ij} \quad i, j \in \mathbb{N}$ in the network at the time t that represents the individuals of a group;
- $\mathcal{L}_t : \mathcal{V}_t \to \mathcal{V}_t$ is the mapping rule that assigns elements of $\mathcal{V}_t$ to each node of $\mathcal{V}_t$; and
- $\mathcal{C}_t : \mathcal{V}_t \to \mathcal{X}$ is the mapping rule that assigns to each node of $\mathcal{V}_t$ a set of states $\mathcal{X}$.

Function $\mathcal{L}_t$ assigns elements of $\mathcal{V}_t$ to each node. Thus, given the node $v_{ij} \in \mathcal{V}_{t-1}$ $\mathcal{L}_t$ assigns a list of nodes $[v_{lm}] \in \mathcal{V}_{t-1}$ connected with v_{ij}, defining the topology of $\mathcal{V}_t$. The assigned nodes can be occupied by individuals in any health state or simply be empty. For example, given a square grid and a *Moore neighbourhood*, $\mathcal{L}_t$ assigns $(2\,r + 1)^2 - 1$ nodes to each one of $\mathcal{V}_t$. The radius r defines de size of node neighbourhood where candidates nodes lay, restricting the network area where nodes can connect with v_{ij}. For example, if homogeneous contacts are required by the epidemic model, like in population-based models, $r = N$ such that each node v_{ij} can contact any other in the grid. In this way, any individual can interact with any other. On the other hand, if $r < N$ each node v_{ij} can only connect with $(2\,r + 1)^2 - 1$ different nodes located in any place of the network, interacting with a limited number of individuals.

Connections distribution is controlled through the probability function employed to establish connection between nodes. For example, if random contact is required, the connections are assigned using an uniform probability distribution. In another cases, an specific probability distribution for each problem can be proposed.

Network states and topologies are updated through repetitive processes of rewriting network blocks (see Figure 4). These process comprise three steps: i) removes a part of

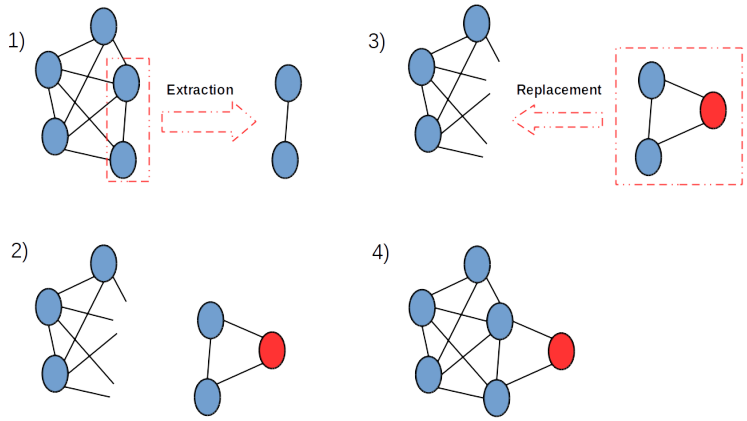

Figure 4: Network rewriting process: 1) extraction; 2) modification and 3) replacement mechanisms.

the network, a sub-net that will be subject of changes; *ii*) produces a new sub-net that will replace the selected one; and *(iii)* reconnect the new sub-net to the rest of the network. These processes are associated with corresponding operations that determine the temporal evolution of network models:

- An **extraction mechanism** that determines which part of the network is selected for upgrading. It is a function that takes the entire network configuration and returns a specific network segment that will be modified;
- A **reshaping mechanism** that produces a new network segment from the selected one, establishing new nodes mapping. It is a function that takes the original configuration and returns a new one with the corresponding links between nodes; and finally
- A **replacement mechanism** that reconnects the new network segment to the network. It is a function that takes the new segment and the network topology and returns the new network topology.

An additional operation must be included (**initial configuration**) to define the initial configuration of the network.

2.3. Health state

Health state determines the epidemiological state of each individual along the epidemic process. It can be designed using different tools, depending on the modelling requirements and information available. The tools employed can range from differential equations to logical rules, finite state automaton and models of agent immune–response. The only requirement of the model is the inclusion of all relevant information available of the disease.

The most common modelling tool is the finite state automaton (or its continuous counter part: the ordinary differential equation) that allows to combine in one model stochastic and deterministic states transitions. Furthermore, it allows modelling different epidemiological scenarios (quarantine, vaccination, multiple strains, among others) by modifying the states

sinc(*i*) Research Institute for Signals, Systems and Computational Intelligence (sinc.unl.edu.ar)
L. López, M. Fernández, A. Gómez & L. Giovanini; "An influenza epidemic model with dynamic social networks of agents with individual behaviour"
Ecological Complexity, Vol. 41, 2020.

and transitions and include individuals heterogeneity (defining the automata parameters through distributions [23]), while it retains simplicity and precision.

Formally, a finite state automaton is defined as $\mathcal{A} = (\mathcal{X}, \mathcal{U}, \mathcal{Y}, \mathcal{T}, \mathcal{O}, \mathcal{X}_0)$ where $\mathcal{X} \subseteq \mathbb{N}_{\leq n_x}$ is a finite states set of n_x states and the initial state $\mathcal{X}_0 \in \mathcal{X}$, $\mathcal{U} \in \mathbb{R}^{n_u}$ is the input set with n_u inputs, $\mathcal{Y} \subseteq \mathcal{X}$ is the output set, $\mathcal{T} : \mathcal{X} \times \mathcal{U} \to \mathcal{X}$ is the transition function and $\mathcal{O} : \mathcal{X} \to \mathcal{Y}$ is the output function. The transition function $\mathcal{T}(x_t, u_t)$ determines which will be the next state (x_{t+1}) given the current state (x_t) and input (u_t). It can be deterministic or stochastic and it can be represented as a transition matrix or a difference equation. The output function $\mathcal{O}(x_t)$ determines which will be the automata output to interact with other agents [24].

3. Study Case

3.1. Spanish Flu

In section 2 we introduce the framework describing the different blocks that characterize an individual's behaviour and their relationship for modelling epidemic situations. In this section, we introduce a study case where we model a Spanish flu epidemic. Here we provide a description of the tools used to model the different aspects of the agent's behaviour for this disease. The models used for each block are:

- **Individual behaviour** is implemented through a FCM;
- **Social behaviour** is implemented through a cellular automaton; and
- **Health state** is implemented through a Moore machine.

3.1.1. Individual behaviour

The individual behaviour is modeled through a FCM based on the model proposed by Mei et al. [22], where the concepts $C_i \quad i = 1, ..., 10$, are divided into three groups:

i) **Input concepts** represent the agent's perceptions of the the environment (*primary emotions*) where C_1 is the number of near infected individuals, C_2 is the number of near recovered individuals and C_5 is the knowledge of the global epidemic situation;

ii) **Internal concepts** represent emotions and feelings of an individual (*secondary emotions*) where C_3 is the health state of individual (provided by health state block), C_4 is knowledge of local epidemiological situation, C_6 is the assessment of local and global epidemiological situation, C_7 is optimism level, C_8 is the memory of similar situations and C_9 are the instant reactions;

iii) **Output concepts** correspond to the senior emotions ($C_{10} \in \mathbb{R}$) representing the actions taken by the agent as a result of a decision process. It controls the number of contacts made by each agent within the contact space, affecting the effective contact rate; and

iv) **Inputs** u_i correspond to the information acquired from agent's neighbourhood where $u_1 \in \mathbb{N}$ is the density of infected and $u_2 \in \mathbb{N}$ is the density of recovered individuals that connected within the neighbourhood of the agent; $u_3 = x_t \in \mathcal{X}$ is the agent current health state and $u_4 \in \mathbb{R}$ is the knowledge of the local epidemiological situation.

sinc(*i*) Research Institute for Signals, Systems and Computational Intelligence (sinc.unl.edu.ar)
L. López, M. Fernández, A. Gómez & L. Giovanini; "An influenza epidemic model with dynamic social networks of agents with individual behaviour"
Ecological Complexity, Vol. 41, 2020.

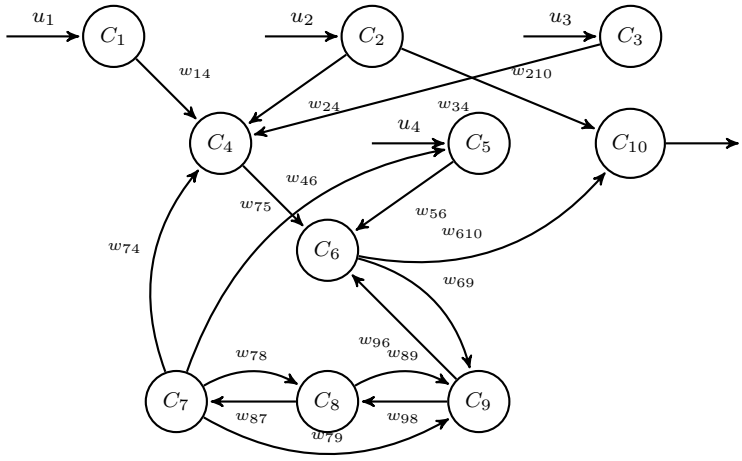

Figure 5: Fuzzy Cognitive Map of the individual behaviour for flu epidemics.

Figure 5 shows the connections between the concepts C_i and inputs u_i with the associated weights $w_{ij} \in W$. The values of the input concepts C_1 and C_2 are estimated at each iteration as the density of infected and recovered individuals within the neighborhood of size ν. The value of the concept C_3 is given by the agent health state lock, which is the output of the health state block (see Figure 3). The value of C_{10} quantifies the individual's perception of the overall epidemiological situation. Here this concept limits the degree of the node as $\lceil (1 - C_{10})\ \nu \rceil$. In this way, the network topology is modified by the FCM since C_{10} determines the degree of connection of each agent, influencing the network topology. Appendix A presents a full description of the FCM threshold functions and training algorithm.

3.1.2. Social behaviour

Social behaviour is implement through a cellular automaton is rectangular, with a Moore neighbourhood of size ν and the neighbourhood radius r, which is used to define the connection degree of each node, are estimated together with the other parameters of the epidemic model. The boundary condition is fixed with a contour composed of empty non-interacting nodes.

Connections between nodes are bidirectional, isotropic and equal at any point of the neighbourhood, providing an input to each node in state S. The input is a value $\lambda \in [0, 1]$ from connected nodes in state I or A. It is used to compute the transition probability to state E. Since S nodes are included in several connections with infectious individuals at any time t, nodes will have as many opportunities to change state as the number of contacts. Since random homogeneous contacts is modelled, like in population-based models, the parameters of the cellular automaton are setting as follows:

- Neighbourhood radius r is estimated with the remaining parameters with constrained by $r < N$; and
- Connections to other nodes are assigned randomly using uniform probability distribution.

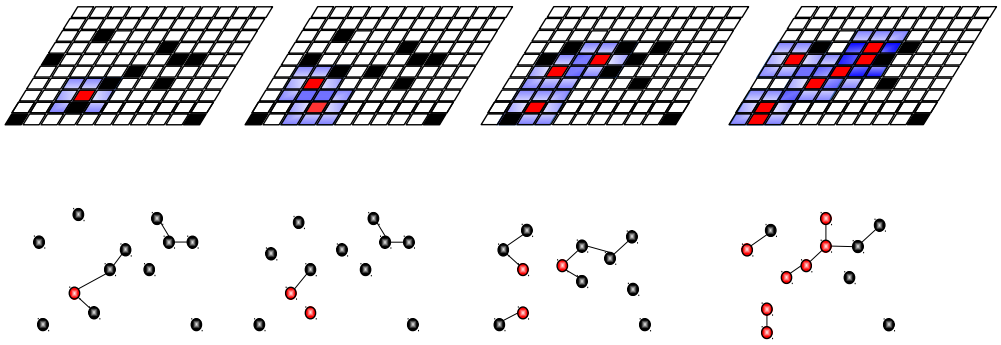

Figure 6: Different representations of the grid: (top) cellular automata and (bottom) boolean network.

Figure 6 provides a detailed insight into the time evolution (dynamics) of the network. Infected individuals are represented by red cells, while healthy individual are represented by black cells. Their neighbourhood is represented through blue cells that defines the influence of each node. The top figure shows the evolution of the cellular automata along time, while the bottom figure shows the evolution of the corresponding boolean network.

3.1.3. Health state

The health state of the agent is modelled using a Moore automata with $\mathcal{X}$ comprises six ($n_x = 6$) epidemic states: susceptible S, exposed E, infectious symptomatic I and asymptomatic A, recovered R and dead D ($\mathcal{X} = \{S, E, I, A, R, D\}$). The initial condition $\mathcal{X}_0$ of each individual is defined stochastically with a high probability of been in state S. The initial population of agents in states E and I si given by N_e and N_i respectively. The automaton has only one input ($n_u = 1$) $\lambda \in \mathbb{R}_{[0,1]}$ emitted by neighbours in state I or A. The input λ becomes active only when the automaton is in state S and it takes into account the neighborhood size ν.

The output function $\mathcal{O}(x_t) = \omega\, x_t$ only computes the infection rate if the automata is in state I ($\omega = \beta$) or A ($\omega = q\,\beta$), where β is the probability of transmission and q is the rate of infection of asymptomatic individuals.

Figure 7 shows the state transition graph of the automaton that models the health state.

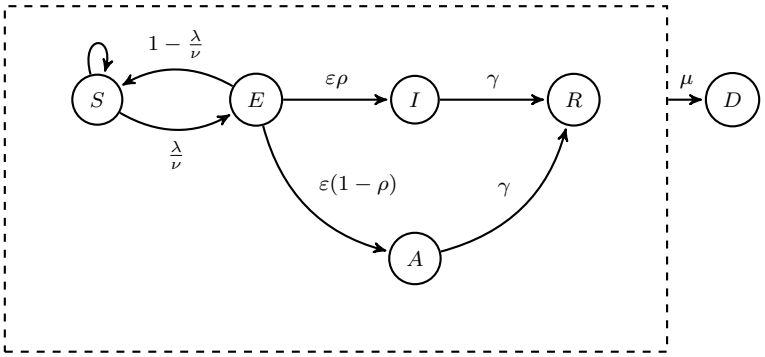

Figure 7: State graph of the health states model.

The automaton combines probabilistic transitions that depend on the input for the first two states ($S \to S$, $S \leftrightarrows E$), which incorporates the stochastic nature of the contagion process, with deterministic transitions for the remainder states ($E \to I \to R$, $E \to A \to R$). The transition between states are defined by the following parameters: the diagnosed rate ϵ, the proportion of reported infectious ρ, the recovery rate γ and the probability of natural death μ. The transition function $\mathcal{T}(x_t, u_t)$ is implemented through a matrix derived from the state transition graph (Figure 7), resulting in the transition matrix shown in Table 1. It is applied in two steps: firstly, the health state block modifies its state due to an active input or disease evolution (Table 1), and then the social behaviour block modifies the contact network, due to the effect of health state and perceptions. If movement is not executed, then the second step is not performed.

Table 1: State transition matrix

	S	E	I	A	R
S	$1-(\mu+\lambda/\nu)$	$1-\lambda/\nu$	0	0	0
E	λ/ν	$1-(\varepsilon+\mu)$	0	0	0
I	0	0	$1-(\gamma+\mu)$	0	γ
A	0	0	0	$1-(\gamma+\mu)$	γ
R	0	0	0	0	$1-\mu$
D	μ	μ	μ	μ	μ

The initial condition $\mathcal{X}_0$ the initial state of the automaton, and it is given by

$$\mathcal{X}_0 = \langle S_i/G_T, E_i/G_T, I_i/G_T, A_i/G_T, R_i/G_T \rangle \tag{1}$$

where G_T is the total number of cells in the grid, S_i, E_i, I_i, A_i, R_i and D_i are the initial number of individuals in each state in the grid (Its sum being equal to G_T and not to the total population, since D_i includes the empty cells). In our case, we only consider probabilities for states S, E, I and D and the cells that are left empty accordingly. All other states do not have initial individuals.

3.2. Parameters estimation

To evaluate the proposed model the epidemic Spanish flu in the Swiss canton of Geneva in 1918 [25] is analised. The model parameters were estimated following a two-step procedure: firstly, a global stochastic optimization method (simulated annealing [26]) is used to perform a *global search* over parameter space looking for good candidates, and then a gradient-based optimization algorithm [27] is used to perform a *local search* over candidate regions to find the best parameters. Stochastic–based–optimization methods generally provide good starting points for gradient–based–optimization methods. The objective function used was the normalized square error (*NMSE*)

$$NMSE = \sum_{k=1}^{m} \frac{\| m_I(k) - d_I(k) \|_2^2}{\| m_I(k) \|_2^2}, \tag{2}$$

sinc(*i*) Research Institute for Signals, Systems and Computational Intelligence (sinc.unl.edu.ar)
L. López, M. Fernández, A. Gómez & L. Giovanini; "An influenza epidemic model with dynamic social networks of agents with individual behaviour"
Ecological Complexity, Vol. 41, 2020.

Table 2: Model parameters

β	ρ	γ	α	q	N_e	N_i	r
8.3	0.087	0.246	0.465	0	207	136	3

where $m_I(k)$ are the number of infected predicted by the model and $d_I(k)$ are the data collected during the epidemic. Table 2 shows the est parameters of the model.

For training the FCM we use the algorithm proposed by Mei [22]. The value of each concept is computed taking into account the influence of other concepts over the specific concept taking into account the value of causal relationships between them. Since we are modelling a local outbreak (city level), the value of $C_5 = 0.5$ is the equivalent to a phase 4 alert according to the World Health Organization and was kept constant along the epidemic process. It is characterized by verified human-to-human transmission at community-level. Another aspect to consider is the threshold function to use in for the actualization of concepts C_i. Since the domain and range of threshold function are known and bounded, a linear function is employed because it considers the ends of the inference interval and retains the same slope in that interval [21]. The threshold function employed to model the Spanish flu is

$$f(x) = \frac{1}{2}\left(\frac{\frac{1}{2}\,x}{(\rho_1 + \rho_2\|W\|)n^{1/2}} + 1\right), \tag{3}$$

where ρ_1 and ρ_2 are values in $[0, 1]$, W is the weight matrix W is given by

$$W = \begin{pmatrix} 0 & 0 & 0 & 0.34 & 0 & 0 & 0 & 0 & 0 & 0 \\ 0 & 0 & 0 & -0.14 & 0 & 0 & 0 & 0 & 0 & -0.34 \\ 0 & 0 & 0 & 0.44 & 0 & 0 & 0 & 0 & 0 & 0 \\ 0 & 0 & 0 & 0 & 0 & 0.52 & 0 & 0 & 0 & 0 \\ 0 & 0 & 0 & 0 & 0 & -0.05 & 0 & 0 & 0 & 0 \\ 0 & 0 & 0 & 0 & 0 & 0 & 0 & 0 & 0.85 & 0.37 \\ 0 & 0 & 0 & -0.13 & -0.27 & 0 & 0 & -0.03 & -0.25 & 0 \\ 0 & 0 & 0 & 0 & 0 & 0 & -0.21 & 0 & -0.07 & 0 \\ 0 & 0 & 0 & 0 & 0 & -0.14 & 0 & 0.09 & 0 & 0 \\ 0 & 0 & 0 & 0 & 0 & 0 & 0 & 0 & 0 & 0 \end{pmatrix}$$

, and n is the number of concepts.

3.3. Model Validation

Model validation is one of the most important steps in the model development. On one hand, graphical methods illustrate a wide range of complex aspects of the relationship between the model and observed data. Figure 8 shows the responses of the proposed model and the *SEIR* model developed by Chowel et al. [25]. In this figure we can see that both models capture the overall dynamic. However, only the proposed model is able of capturing the initial stage of the epidemic process, where the *SEIR* model fails to reproduce the observed data. The proposed model is also able of correctly estimating the magnitude and time of the epidemic peak. On the other hand, the *SEIR* model sub estimates the magnitude of the peak and overestimates its time of occurrence. Both models fail to reproduce the data variability at the end of the epidemic process (infected waves around at days 55 and 65). The error was computed according to $NMSE$ function for both models, resulting in $NMSE = 3.3$ for the *SEIR* model and $NMSE = 1.6$ for the proposed model.

sinc(*i*) Research Institute for Signals, Systems and Computational Intelligence (sinc.unl.edu.ar)
L. López, M. Fernández, A. Gómez & L. Giovanini; "An influenza epidemic model with dynamic social networks of agents with individual behaviour"
Ecological Complexity, Vol. 41, 2020.

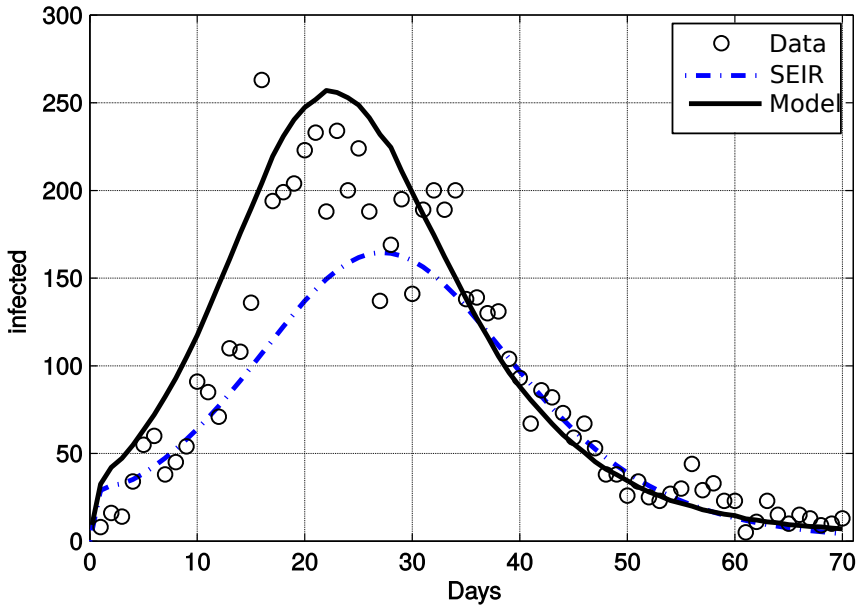

Figure 8: Model fitting.

The model was also numerically validated using the *Akaike Information Criterion* (AIC), which provides a measure of model quality considering both accuracy and complexity simultaneously. This approach is widely used to measure the quality of models and validate them [28]. The AIC criterion is equivalent to a cross-leave-one-out in longitudinal data models validation [29]. Models that have an AIC within the range $1-2$ consistently support structural variation in the data. The models that have their value in the range $3-7$ withstand significantly structural variation in the data. Finally, those models that have $AIC > 10$ do not explain structural changes in the data. The AIC index is computed as follows

$$AIC = log\left(det\left(\frac{1}{m}\sum_{1}^{m}\varepsilon(t,\Theta)(\varepsilon(t,\Theta))^{T}\right)\right) + \frac{2n}{m}, \tag{4}$$

where Θ is the set of n estimated parameters m is the number of samples and $\varepsilon(t,\Theta)$ is the measured error. The AIC was chosen instead of *Bayesian Information Criterion* (BIC) because the AIC is an estimate of the relative distance between the true dynamic function and the model dynamic, plus a constant, while BIC is an estimate of the posterior probability of a model considered true under some Bayesian configuration. A lower AIC represents a model closer to true dynamic. The AIC index of the proposed model is 6.1, while the AIC of the *SEIR* model is 7.5. The proposed model behaves robustly to structural variation of the data.

Finally, the statistical significance of these results was assessed by calculating the probability of error in the approach of both model. The results show that the proposed model is better than the *SEIR* (see Table 3). For this test, statistical independence of errors ad-

sinc(*i*) Research Institute for Signals, Systems and Computational Intelligence (sinc.unl.edu.ar)
L. López, M. Fernández, A. Gómez & L. Giovanini; "An influenza epidemic model with dynamic social networks of agents with individual behaviour"
Ecological Complexity, Vol. 41, 2020.

justment for different data sets is assumed and the errors of a binomial distribution are approximated with a Gaussian distribution. One of the fundamental aspects of the model evaluation is to estimate the probability of error, because

- It allows to evaluate the usefulness of the model for the intended purposes;
- It allows to compare their performance against other models.

Three new data sets were generated with gaps randomly chosen with uniform probability: *i*) a data set with $n = 10$ data points removed, *ii*) a data set with $n = 20$ data points removed and *iii*) a data set with $n = 30$ data points points. Both models were trained with each data set to get seven generations of parameters for each model. Then, we perform 1000 simulations for each generation of parameters obtained in the previous step in order to obtain a good approximation of the average response. Finally, the average error for each is calculated taking into account the average response model using data that was extracted from the original data set. Thus for each set of adjustment parameters with different gaps in the data set that the proposal we hypothesize that $P(Error_{model} < Error_{SEIR}) > p$.

Table 3: Significance of the error for the model

10 gaps data set				
model	Error	μ	σ	$P(p_1 < p_2)$
Proposed model	8.09	0.919	0.0044	99.96
SEIR model	10.04	0.896	0.005	
20 gaps data set				
model	Error	μ	σ	$P(p_1 < p_2)$
Proposed model	5.01	0.95	0.0035	94.15
SEIR model	5.75	0.943	0.0038	
30 gaps data set				
model	Error	μ	σ	$P(p_1 < p_2)$
Proposed model	4.9	0.951	0.0035	97.23
SEIR model	5.88	0.941	0.0038	

Table 3 shows the results for statistical significance for the different validation sets. It can be seen that the proposed model is better than the *SEIR*, having confidence intervals error above of 90%.

3.4. Results and discussion

In this section, different epidemiological situations and control strategies are studied, through modification of the model blocks, in order to assess the capabilities of the proposed framework to model different epidemiological scenarios.

3.4.1. Population heterogeneity

The use of a constant rate of infection does not consider the role of individuals variation in the infection process. This variability can have a great influence when the spatial distribution is not uniform and there is a significant presence of superspreaders [9, 30]. The individual reproductive number β, the expected number of secondary cases can be described

sinc(*i*) Research Institute for Signals, Systems and Computational Intelligence (sinc.unl.edu.ar)
L. López, M. Fernández, A. Gómez & L. Giovanini; "An influenza epidemic model with dynamic social networks of agents with individual behaviour"
Ecological Complexity, Vol. 41, 2020.

through continuous distribution functions instead of constant parameters. If the infectivity of individuals is continuously distributed, heterogeneity can be added to the model. These variability in reproductive number may be due to factors such as undiagnosed infected individuals, high rates of contact or high viral load in some infected individuals, among others. In order to take in account this factor, among others.

One situation is a population with a majority of individuals having similar degree of infectivity and minority with a higher variability. To incorporate this fact into the model, the parameter β for each individual is determine from a normal distribution defined through a mean ($\bar{\beta}$) and the parameter variance (σ_β). These parameters were estimated together with the others parameters of the model, resulting in $\bar{\beta} = 8.3$ and $\sigma_\beta = 0.2$. Another situation is a population with two dominant groups of individuals with different degree of infectivity and minority with a higher variability is generated. To incorporate this fact into the model, the parameter β for each individual is determine from a bimodal distribution defined through distribution with two modes β_I and β_S. These parameters were estimated together with the others parameters of the model resulting in $\beta_I = 8.3$ and $\beta_S = 8.7$, corresponding to the infection rate through contact with infected individuals and superspreaders respectively.

Figure 9 shows the temporal dynamics of infected individuals for the model incorporating population heterogeneity. When more heterogeneity is added to the model, the model closely approximates the real data. In this figure can see that both models capture the overall dynamic of the epidemic. However, only the model with the bimodal distribution is able of

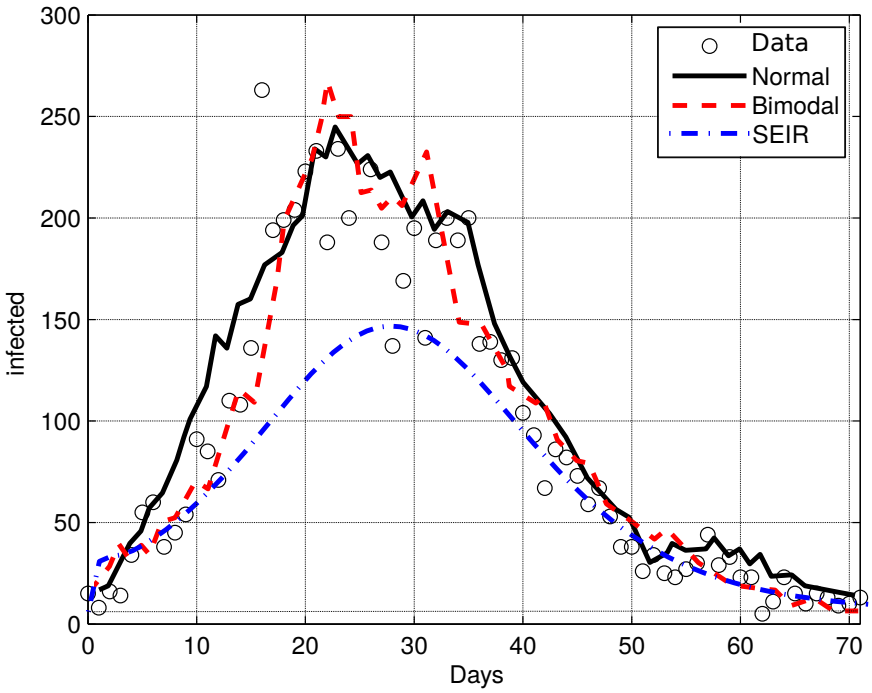

Figure 9: Temporal dynamics for heterogeneous infectivity.

properly capture the stages previous and after the epidemic peak of the epidemic process. The model with the normal distribution overestimates the number of cases during a similar period, however it is able of modelling the small epidemiological waves at the end of the epidemic process (infected waves around at days 55 and 65). The error was computed according to $NMSE$ function, resulting in $NMSE = 3.3$ for the *SEIR* model, $NMSE = 1.8$ for the proposed model with normal distribution and $NMSE = 1.7$ for the proposed model with bimodal distribution. The numerical analysis of these cases showed an $AIC = 6.3$ index when infectivity is modelled by a normal distribution and $AIC = 6$ when infectivity is modelled as a bimodal distribution.

3.4.2. Multiple strains

One way of modelling epidemics with multiple relate strains of a virus is adding to $\mathcal{X}$ a new state that incorporates the cross-immunity effect (C), which introduces an intermediate state between susceptible and recovered state. In this new state, the individual is exposed to a strain antigenically similar but different that can be controlled by the immunity acquire through the original strain (Figure 10).

For a dominant strain, individuals can be found in any of the following states: Susceptible (S) when it is fully susceptible to both strains; Exposed (E) after a contact with an infectious individual that is incubating the disease; Infectious (I) when it is infected by any strain; Recovered (R) when he is fully recovered and cross-immune (C) when it is recovered but is susceptible to secondary strains. The dynamics of the health state takes into account the fact that after recovering from the infection, individuals can obtain partial immunity to the secondary strain. Individuals who are in R have recovered from the main strain and they have full immunity against this strain, but after a period of time they go to a state C since they only have partial immunity to the new strain. While individuals that are in C, they are exposed to the same strain of individuals who are in I, only a smaller fraction of them is infected. With this approach, individuals who are in the R state are assumed completely immune. The parameters that determine the transitions between C and S, E and R (γ, δ, β and σ respectively) are determine from a distribution in order to

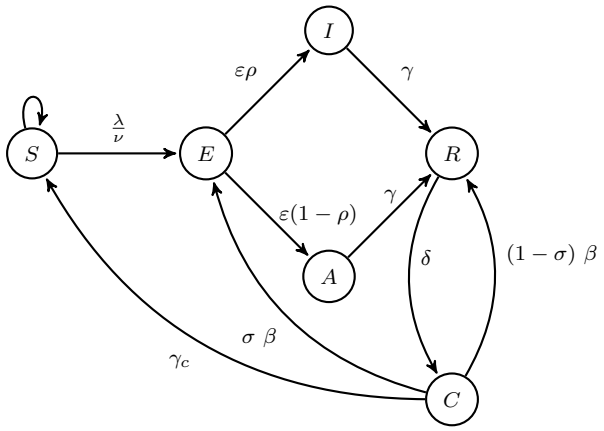

Figure 10: State graph of the epidemic model for multiple strains.

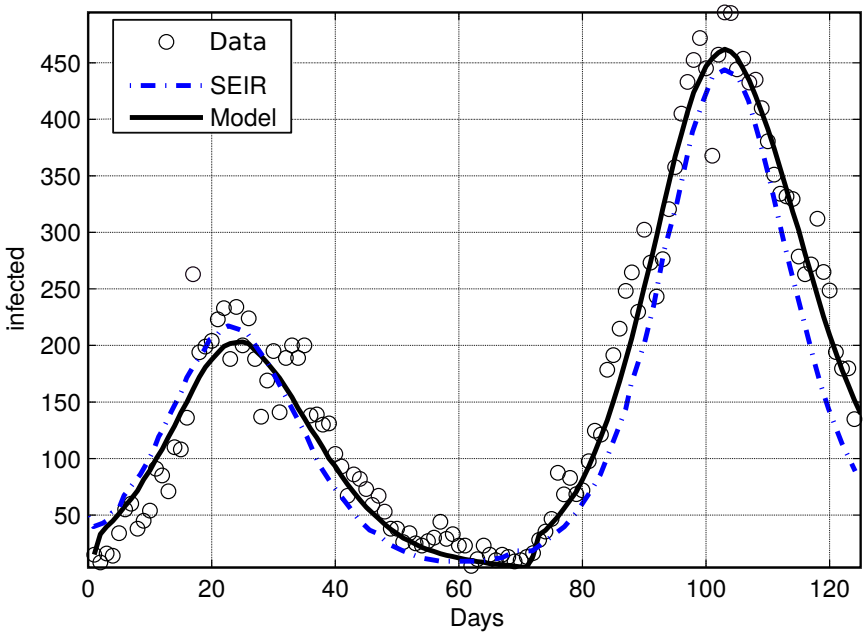

Figure 11: Temporal dynamic for multiple strain model.

incorporate their variability within the population assuming uniform distribution for all the parameters, defining the parameter distributions as the limits of the interval (initial and final value). These parameters were estimated together with the others parameters of the model, resulting in $\gamma \in [0.1, 0.2]$, $\delta \in [0.2, 0.4]$ and $\sigma \in [0.05, 0.09]$.

Figure 11 shows the responses of the proposed model and the *SEIR* model developed by Rios-Doria and Chowel [31]. In this figure we can see that both models capture the overall dynamic of both epidemic waves, predicting properly the time and magnitude of epidemic peak. The *SEIR* model perform better in the initial stages of the first wave, while the proposed model only fail to predict the magnitude of the first wave peak. Both models fail to reproduce the data variability at the end of the first epidemic wave (infected waves around from days 55 and 70). The error was computed according to $NMSE$ function for both models, resulting in $NMSE = 3.5$ for the *SEIR* model and $NMSE = 1.5$ for the proposed model. The numerical analysis of these cases showed an $AIC = 6.4$ index for the proposed model and $AIC = 7.7$ index for the *SEIR* model.

3.4.3. Vaccination and quarantine

Vaccination is considered the most successful and cost-effective intervention policy to reduce both morbidity and mortality of individuals. The resulting dynamics from implementing this intervention can be captured by adding a new state to $\mathcal{X}$. Let's call this state V, or vaccinated. Individuals who are in this state have a lower φ probability than those who have not been vaccinated infection.

While the influenza vaccine is an accurate way to prevent the disease, protection can vary

sinc(*i*) Research Institute for Signals, Systems and Computational Intelligence (sinc.unl.edu.ar)
L. López, M. Fernández, A. Gómez & L. Giovanini; "An influenza epidemic model with dynamic social networks of agents with individual behaviour"
Ecological Complexity, Vol. 41, 2020.

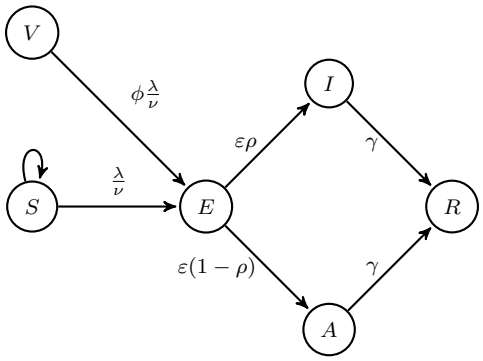

Figure 12: State graph of the epidemic states for vaccination model.

widely depending on who is given the vaccine, plus how well the influenza vaccine match the viruses in circulation. In general, the influenza vaccine has the greatest effect on healthy adults and elder children. Some individuals may develop weaker immunity than others after vaccination. However, even for these individuals, the influenza vaccine can provide some protection. In order to consider these factors in the model, it is established that vaccinated individuals are less likely than non-vaccinated susceptible individuals to contract the disease.

In Figure 12 the Moore machine that models this epidemiological situation is introduced. In order to evaluate the variability in vaccine efficiency, the φ parameter can be taken in a range of $[0.45, 0.65]$ following uniform probability distribution. To carry out the experiment the population is initialized with a variable number of vaccinated individuals. From the point of view of a contact network, vaccinate an individual means changing the influence of a node over neighbouring nodes. By increasing the percentage of vaccinated individuals in the population decreases the influence that infectious nodes have on susceptible nodes.

Figure 13 shows the results of how vaccination affects the temporal dynamics of the disease when increases the percentage of individuals in the population who are vaccinated. As is intuitive thinking, by vaccinating individuals in the population, the likelihood of effective contacts is reduced. From the point of view of a network, this practice is equivalent to saying that certain network nodes (vaccinated individuals) represent obstacles by which the pathogen can not circulate and spread through the rest of the network.

Isolation and quarantine help to protect the population by preventing exposure to people who have or may have a disease. The isolation separates people sick with a contagious disease of people who are not sick. Quarantine separates and restricts the movement of people who were exposed to a communicable disease to see if they get sick.

Classical models assume that the practice of this health policy is not 100% effective, so it is contemplated that the population quarantining can infect susceptible population at a lower rate than the infectious population not start quarantine. In the case of networking based model this hypothesis, it is also true. While not explicitly contemplated as a new element in the set $\mathcal{X}$, individuals quarantined tend to reduce their number of contacts in order to no longer influence the individuals who are within its range of influence. To model this, we suppose that it is not realistic to assume a total quarantine, so we fix a random

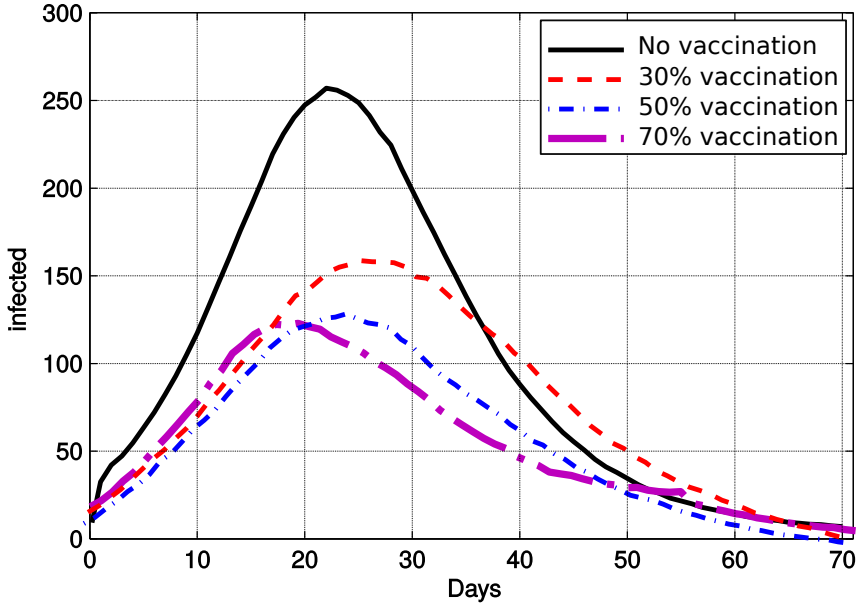

Figure 13: Temporal dynamics for different vaccinated levels.

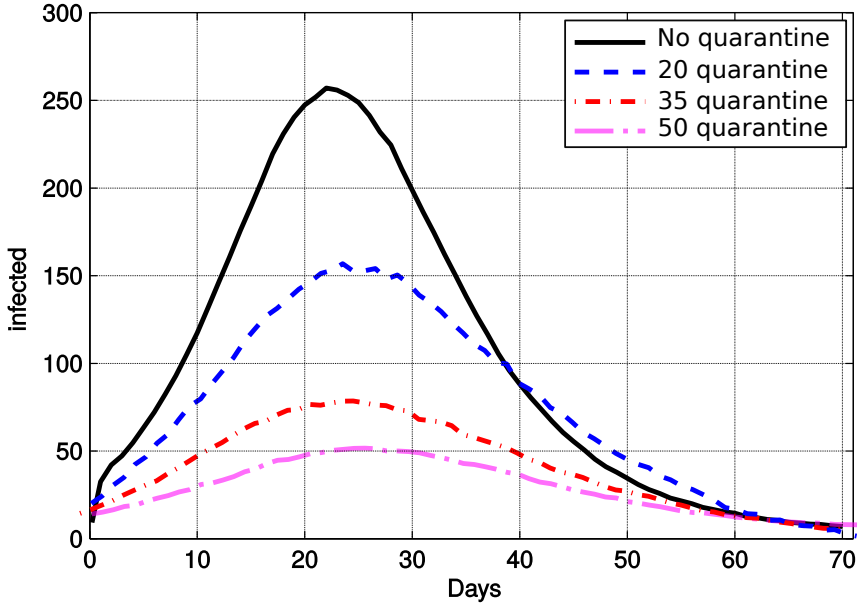

Figure 14: Temporal dynamics for different quarantine periods.

variable ω which takes values in the interval $[0.4, 0.5]$ and the number of contacts the is determined by $\lceil (1-\omega)\ \nu \rceil$. Which means that each individual reduces their number of contacts between 60% and 50%. On the other hand, the movement of individuals in the contact space is limited. Thus, although the circulation of infectious agents is limited in the global network, locally the pathogen may continue to be circulating that it is likely to reach an infected individual.

Figure 14 shows the evolution of the temporal dynamics for different quarantining stages. When individuals are quarantined cannot move freely through the network, this equates to the network topology remains constant in certain areas from the instant of time in which this practice is implemented, as result, infected individuals do not spread the disease as the number of contacts you have decreases when the movement is reduced.

4. Conclusions

This paper addressed the problem of epidemic modelling through an individual-based approach. These models represent a modelling framework significantly different from that proposed by models based on traditional individuals because the way we model individual's behaviour. The classic way of implementing this type of model is to represent it through a set of rules. In this paper, we propose to model the behaviour of individuals through the aggregation of three behavioural blocks. In this way, individualized interactions and infections define the spread of disease at the population level.

Although, to date, a large number of studies have been implemented using modelling based on individuals to model different diseases. The different approaches may vary considerably and there is no unified conceptual framework for the implementation of models based on individuals. On the other hand, there are a large number of software tools, platforms and libraries that allow implementing all kinds of models but these are applications and not a formal framework.

The conceptual framework presented proposes the construction of a model based on individuals through a modular approach. The dynamics of the individual is a consequence of the behaviour of the individual. The behaviour is constructed from three units: Individual Behaviour; Social Behaviour and the Health State. In this way, the modules can be separately implemented using different modelling techniques. The overall dynamics of the system arises as a result of the adaptive network behaviour.

In order to validate the proposed model, we addressed the problem of modelling an influenza epidemic using a network of contacts that allow obtaining good approximations of the temporal dynamics that characterize this type of epidemics and make possible to see the social dimension of the phenomenon through the contact between the actors of the network.

The proposed framework also allows modelling different situations such as quarantine, vaccination or multiple strains epidemic changing behaviour modelling unit (individual) or social behaviour such as quarantine. The importance of the framework presented in this work lies in the fact that it is possible to model the dynamics of complex systems through the logic of self-organized emerging systems.

sinc(*i*) Research Institute for Signals, Systems and Computational Intelligence (sinc.unl.edu.ar)
L. López, M. Fernández, A. Gómez & L. Giovanini; "An influenza epidemic model with dynamic social networks of agents with individual behaviour"
Ecological Complexity, Vol. 41, 2020.

5. Acknowledgements

The authors would like to thank National University of Litoral (UNL) and the Research Institute for Signals, Systems and Computational Intelligence (sinc(i)), Santa Fe, Argentina and the National Scientific and Technical Research Council, Argentina. This work has been funded by the National Scientific and Technical Research Council.

References

[1] D. Bernoulli, An Attempt at a New Analysis of the Mortality Caused by Smallpox and of the Advantages of Inoculation to Prevent it, 1760.

[2] M. J. Keeling, P. Rohani, Modeling Infectious Diseases in Humans and Animals, Princeton University Press, 2011.

[3] S. Eubank, H. Guclu, V. S. A. Kumar, M. V. Marathe, A. Srinivasan, Z. Toroczkai, N. Wang, Modelling disease outbreaks in realistic urban social networks, Nature 429 (6988) (2004) 180–184.

[4] I. M. Longini, A. Nizam, S. Xu, K. Ungchusak, W. Hanshaoworakul, D. A. T. Cummings, M. E. Halloran, Containing pandemic influenza at the source, Science 309 (5737) (2005) 1083–1087.

[5] E. Halloran, N. Ferguson, S. Eubank, I. M. Longini, D. A. T. Cummings, B. Lewis, S. Xu, C. Fraser, A. Vullikanti, T. C. Germann, Others, Modeling targeted layered containment of an influenza pandemic in the United States, Proceedings of the National Academy of Sciences 105 (12) (2008) 4639–4644.

[6] D. Balcan, V. Colizza, B. Gonçalves, H. Hu, J. J. Ramasco, A. Vespignani, Multiscale mobility networks and the spatial spreading of infectious diseases, Proc. Natl. Acad. Sci. U. S. A. 106 (51) (2009) 21484–21489.

[7] D. L. Chao, M. E. Halloran, V. J. Obenchain, I. M. Longini, Jr, FluTE, a publicly available stochastic influenza epidemic simulation model, PLoS Comput. Biol. 6 (1) (2010) e1000656.

[8] S. Merler, M. Ajelli, A. Pugliese, N. M. Ferguson, Determinants of the spatiotemporal dynamics of the 2009 H1N1 pandemic in Europe: implications for real-time modelling, PLoS Comput. Biol. 7 (9) (2011) e1002205.

[9] J. O. Lloyd-Smith, S. J. Schreiber, P. E. Kopp, W. M. Getz, Superspreading and the effect of individual variation on disease emergence, NATURE-LONDON- 438 (7066) (2005) 355.

[10] R. Pastor-Satorras, C. Castellano, P. Van Mieghem, A. Vespignani, Epidemic processes in complex networks, Rev. Mod. Phys. 87 (3) (2015) 925–979.

[11] R. F. Arthur, E. S. Gurley, H. Salje, L. S. P. Bloomfield, J. H. Jones, Contact structure, mobility, environmental impact and behaviour: the importance of social forces to infectious disease dynamics and disease ecology, Philos. Trans. R. Soc. Lond. B Biol. Sci. 372 (1719).

[12] R. Cohen, S. Havlin, Complex Networks: Structure, Robustness and Function, Cambridge University Press, 2010.

[13] M. Newman, Networks: An Introduction, OUP Oxford, 2010.

[14] T. Gross, B. Blasius, Adaptive coevolutionary networks: a review, Journal of the Royal Society Interface 5 (20) (2008) 259–271.

[15] A. Damasio, Descartes error: Emotion, reason, and the human brain, New York: Putnam.

[16] J. E. Laird, A. Newell, P. S. Rosenbloom, Soar: An architecture for general intelligence, Artificial intelligence 33 (1) (1987) 1–64.

[17] J. R. Anderson, D. Bothell, M. D. Byrne, S. Douglass, C. Lebiere, Y. Qin, An integrated theory of the mind., Psychological review 111 (4) (2004) 1036.

[18] J. Gratch, S. Marsella, A domain-independent framework for modeling emotion, Cognitive Systems Research 5 (4) (2004) 269–306.

[19] J. D.-P. B. Xiao-Juan, Y. Y.-X. S. Wei-Ren, Research on emotion theory and the decision models based on emotion, Computer Science 4 (2007) 042.

[20] P. Battaglia, R. Pascanu, M. Lai, D. J. Rezende, et al., Interaction networks for learning about objects, relations and physics, in: Advances in neural information processing systems, 2016, pp. 4502–4510.

[21] Lee, Kim, Cho, Design of activation functions for inference of fuzzy cognitive maps: application to clinical decision making in diagnosis of pulmonary infection, Healthc. Inform. Res. 18 (2) (2012) 105–114.

[22] S. Mei, Y. Zhu, X. Qiu, X. Zhou, Z. Zu, A. V. Boukhanovsky, P. M. A. Sloot, Individual decision making can drive epidemics: a fuzzy cognitive map study, IEEE Trans. Fuzzy Syst. 22 (2) (2014) 264–273.

[23] L. López, G. Burguerner, L. Giovanini, Addressing population heterogeneity and distribution in epidemics models using a cellular automata approach, BMC research notes 7 (1) (2014) 234.

sinc(*i*) Research Institute for Signals, Systems and Computational Intelligence (sinc.unl.edu.ar)
L. López, M. Fernández, A. Gómez & L. Giovanini; "An influenza epidemic model with dynamic social networks of agents with individual behaviour"
Ecological Complexity, Vol. 41, 2020.

[24] A. R. Mikler, S. Venkatachalam, K. Abbas, Modeling infectious diseases using global stochastic cellular automata, J. Biol. Syst. 13 (4) (2005) 421–439.
[25] Chowell, Ammon, Hengartner, Hyman, Transmission dynamics of the great influenza pandemic of 1918 in Geneva, Switzerland: assessing the effects of hypothetical interventions, J. Theor. Biol. 241 (2) (2006) 193–204.
[26] K. Deb, A. Pratap, S. Agarwal, T. Meyarivan, A fast and elitist multiobjective genetic algorithm: NSGA-II, IEEE Trans. Evol. Comput. 6 (2) (2002) 182–197.
[27] R. H. Byrd, J. C. Gilbert, J. Nocedal, A trust region method based on interior point techniques for nonlinear programming, Math. Program. 89 (1) (2000) 149–185.
[28] M. R. E. Symonds, A. Moussalli, A brief guide to model selection, multimodel inference and model averaging in behavioural ecology using akaike's information criterion, Behav. Ecol. Sociobiol. 65 (1) (2011) 13–21.
[29] Y. Fang, Asymptotic equivalence between cross-validations and akaike information criteria in mixed-effects models, J. Data Sci. 9 (1) (2011) 15–21.
[30] A. P. Galvani, R. M. May, Epidemiology: dimensions of superspreading, Nature 438 (7066) (2005) 293–295.
[31] D. Rios-Doria, G. Chowell, Qualitative analysis of the level of cross-protection between epidemic waves of the 1918–1919 influenza pandemic, Journal of Theoretical Biology 261 (4) (2009) 584–592.
[32] B. Kosko, Fuzzy cognitive maps, International journal of man-machine studies 24 (1) (1986) 65–75.

sinc(*i*) Research Institute for Signals, Systems and Computational Intelligence (sinc.unl.edu.ar)
L. López, M. Fernández, A. Gómez & L. Giovanini; "An influenza epidemic model with dynamic social networks of agents with individual behaviour"
Ecological Complexity, Vol. 41, 2020.

Appendix A. Framework implementation

In Figure A.15 the interaction between the different model levels is shown. In this figure can be seen each one of the principal input variables (light blocks) and the output variable resulting from that block (dark blocks).

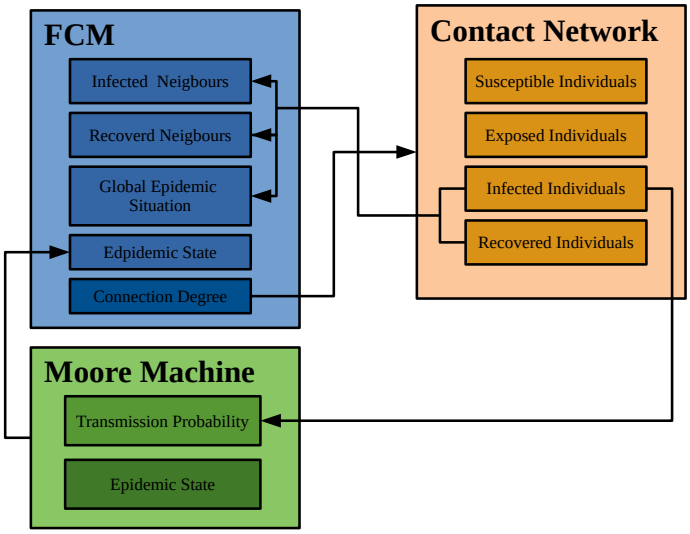

Figure A.15: interaction between model levels. In blue the FCM for individual level, orange the contact network for social behaviour and in green Moore machine (automata) for the epidemic level

Algorithm 1 summarize the in general terms the model implementation. Given the initial configuration of the contact network, the evolution of the system depends on the interaction of each of the blocks that model the behaviour. At first, the number of contacts of each individual is determined by the FCM, then a re-mapping of his contact network through the extraction and replacement algorithms is made and then the health state is updated.

Algorithm 1 Model implementation

$G = \mathcal{M}_{M\times N}\{MxN$ square grid where automate evolve$\}$
N_T {Total individuals}
$N =$ {Total days}
$G = I\{$Initial configuration of the network.$\}$ (Algorithm 2)
for $t = 1 \rightarrow N$ **do**
  for $j = 1 \rightarrow N_T$ **do**
    Individual behaviour actualization j
    Health state actualization and *Reconfiguration of the contact network of* j
  end for
end for

In Algorithm 1 can be seen that for each individual in the network each one of the behavioural blocks is performed. First of all the initialization of the whole system is made as shown in algorithm 2.

The health state actualization is performed in the sub-network extraction step (Algorithm 3) , for each jth individual in the network, algorithms 5, 6 and 7 are performed. thus,

sinc(*i*) Research Institute for Signals, Systems and Computational Intelligence (sinc.unl.edu.ar)
L. López, M. Fernández, A. Gómez & L. Giovanini; "An influenza epidemic model with dynamic social networks of agents with individual behaviour"
Ecological Complexity, Vol. 41, 2020.

Algorithm 2 Initialization algorithm

$G = \mathcal{M}_{M\times N}(\mathbb{R})$ {Contact network is defined}
N_s {Number of susceptible individuals}
N_i {Number of infectious individuals}
N_e {Number of exposed individuals}
N_r {Number of recovered individuals}
for $i \to N_s$ **do**
  $G(x, y) = S,\ 1 \leq x \leq M,\ 1 \leq x \leq N$ {Susceptible individual are distributed in the network}
end for
for $i \to N_i$ **do**
  $G(x, y) = I,\ 1 \leq x \leq M,\ 1 \leq x \leq N$ {Infectious individual are distributed in the network}
end for
for $i \to N_e$ **do**
  $G(x, y) = E,\ 1 \leq x \leq M,\ 1 \leq x \leq N$ {Exposed individual are distributed in the network}
end for
for $i \to N_r$ **do**
  $G(x, y) = R,\ 1 \leq x \leq M,\ 1 \leq x \leq N$ {Recovered individual are distributed in the network}
end for

Algorithm 3 Extraction algorithm

$G_e = \mathcal{M}_{m\times n}(\mathbb{R}) \in G = \mathcal{M}_{M\times N}(\mathbb{R})$ {define the extraction sub-net}
for $g_i \in G_e$ **do**
  Algorithm 5
  Algorithm 6
  Algorithm 7
  Algorithm 8 (if individual movement is simulated)
end for

Algorithm 4 Replacement algorithm

$G_r = \mathcal{M}_{m\times n}(\mathbb{R}) \in G = \mathcal{M}_{M\times N}(\mathbb{R})$ {defines the segment of the network to replace}
$G_r = G_e$

its important to see that the health state configuration is performed before the reconfiguration of the contact network is performed. Individuals health state is calculated in each reconfiguration stage during the individual's contact actualization.

Algorithm 5 Infectious state

if $State = I$ **then**
  if $Neighbor = S$ **then**
    $Z \sim U[0, 1]$
    if $Z < \beta/\nu$ **then**
      $State = E$
    end if
  end if
end if
if $State = A$ **then**
  if $State = S$ **then**
    $Z \sim U[0, 1]$
    if $Z < q\beta/\nu$ **then**
      $State = E$
    end if
  end if
end if

In the reconfiguration of the contact network step, algorithms 3 and 4 are performed in each time step t. The initial configuration of the network (algorithm 2) is fixed at $t = 0$. The individuals movement is performed by the algorithm 8.

sinc(*i*) Research Institute for Signals, Systems and Computational Intelligence (sinc.unl.edu.ar)
L. López, M. Fernández, A. Gómez & L. Giovanini; "An influenza epidemic model with dynamic social networks of agents with individual behaviour"
Ecological Complexity, Vol. 41, 2020.

Algorithm 6 Exposed state

```
if State = E then
    Z ~ U[0, 1]
    if Z < ερ then
        State = I
        if Z < ε(1 − ρ) then
            State = A
        end if
    end if
end if
```

Algorithm 7 Recovery phase

```
if State = I o State = A then
    Z ~ U[0, 1]
    if Z < γ1 then
        State = R
    end if
end if
```

Algorithm 8 Individuals movement

```
Z1, Z2 ~ U[−r, r]
Aux = State(i, j)
State(i, j) = State(i + Z1, j + Z2)
State(i + Z1, j + Z2) = Aux
```

In the individual's behaviour actualization step (Algorithm 1) the FCM concepts are updated giving the input concepts C_1, C_2, C_3 and C_5. The new concepts are computed according to:

$$C_i(t) = f(k_1 \sum_{j=1, j\neq i}^{n} C_j(t-1)w_{ji} + k_2 C_i(t-1)), \tag{A.1}$$

where k_2 is the contribution of the previous value and k_1 is the influence of the related concepts. The two parameters k_1 and k_2 satisfy $0 < k_1, k_2 < 1$ and f is the threshold.

Algorithm 9 was used for the FCM training. For the rule A.2, $\eta \approx 0$ is the learning coefficient, ξ is the loss of the learning coefficient. $F1$ y $F2$ are the termination criteria. The first is the minimization for the Euclidean distance between the current value of the concept of output and the expected value. Taking into account that $C_10 \in [C_{10}^{min}, C_{10}^{max}]$, the value $C_{10}^{expected}$ must be $C_{10}^{expected} = (C_{10}^{min} + C_{10}^{max})/2$. The second rule is used to ensure the convergence of the method after a number of iterations, being $\epsilon \approx 0$.

In order to validate the W matrix used in Section 3.1 we generate $10,000$ vectors X_0, where each $x_i \in [0, 1]$, $i = 1, ..., 10$ using an uniform probability distribution, then we perform the computation of C_{10} using equation A.1. The obtained results re inside the interval $[0.2, 0.8]$ (Figure A.16)

It's also important the used f threshold function used in equation A.1 and algorithm 9. The sigmoid function $f(x) = \frac{1}{1+e^{-kx}}$, is commonly used for this [22, 32], where x is the value of the C_i concept being calculated and k shape coefficient. The coefficient k tends to limit the output values to a very specific range $[a, b]$ .Also the sigmoid function domain $(-\infty, \infty)$, while its range is $(0, 1)$, not including the extremes of the interval. We choose a linear function as a threshold. These functions are particularly useful if when you know the

sinc(*i*) Research Institute for Signals, Systems and Computational Intelligence (sinc.unl.edu.ar)
L. López, M. Fernández, A. Gómez & L. Giovanini; "An influenza epidemic model with dynamic social networks of agents with individual behaviour"
Ecological Complexity, Vol. 41, 2020.

Algorithm 9 Entrenamiento del FCM

(1) $W_0 = w_{ji} \in [-1, 1];\ j, i = 0, ..., 10$ {Set initial weight matrix}
(2) $X_i^0 = x_i^0 \in [0, 1]$ {Set initial concepts}
(3) $x_i(t) = f(k_1 \sum_{j=1, j\neq i}^{n} x_j(t-1) w_{ji} + k_2 x_i(t-1))$ {Get the new concepts}
(4)

$$w_{ji}^t = \begin{cases} 0 & , si\ w_{ji}^{t-1} = 0 \\ \xi w_{ji}^{t-1} + \eta x_i^{t-1}(x_j^{t-1} - \left|w_{ji}^{t-1}\right| x_i^{t-1}) & , si\ w_{ji}^{t-1} \neq 0, \end{cases} \tag{A.2}$$

{Get the new weight matrix}
(5)
if $w_{ji}^t > 1$ **then**
  $w_{ji}^t = 1$
else if $w_{ji}^t < -1$ **then**
  $w_{ji}^t = -1$
end if{ In order to keep $w_{ji}^t \in [-1, 1]$ }
(6)
if $min(F1 = \sqrt[2]{C_{10}^t - C_{10}^{expected}}) \rightarrow$ **true then**
  end algorithm
else if $F2 = \left|C_{10}^{t+1} - C_{10}^t\right| < \epsilon$ **then**
  end algorithm
else
  Back to step 2
end if{check termination criteria}

range x can take values during the inference process [21].

$$f(x) = \frac{1}{2}(\alpha x + 1), \tag{A.3}$$

where α is defined as

$$\alpha = \frac{0.5}{(\rho_1 + \rho_2 \|W\|) n^{1/2}}, \tag{A.4}$$

where $\rho_1 \ \ \& \ \ \rho_2 \ \in \ [0, 1]$ and W is the weigth matrix.

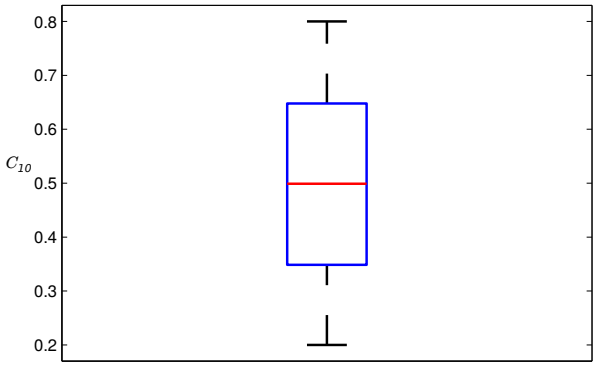

Figure A.16: Box plot for C_{10} output.